Vol. 671: 111–128, 2021
https://doi.org/10.3354/meps13777

MARINE ECOLOGY PROGRESS SERIES
Mar Ecol Prog Ser

Published August 5

Impact of ocean carbonation on long-term regulation of light harvesting in eelgrass *Zostera marina*

Billur Celebi-Ergin[1,2,*], Richard C. Zimmerman[1], Victoria J. Hill[1]

[1]**Department of Ocean and Earth Sciences, Old Dominion University, 4600 Elkhorn Avenue, Norfolk, VA 23529, USA**

[2]***Present address:*** **Department of Molecular Biology and Genetics, Koç University, Rumelifeneri Yolu 34450 Sariyer/Istanbul, Turkey**

ABSTRACT: Seagrasses account for approximately 10% of the total carbon stored in the ocean, although photosynthesis of seagrasses is carbon-limited at present oceanic pH levels. Therefore, increasing atmospheric CO_2 concentration, which results in ocean acidification/carbonation, is predicted to have a positive impact on seagrass productivity. Previous studies have confirmed the positive influence of increasing CO_2 on photosynthesis and survival of the temperate eelgrass *Zostera marina*, but the acclimation of photoprotective mechanisms in this context has not been characterized. We aimed to quantify the long-term impacts of ocean acidification on photochemical control mechanisms that promote photosynthesis while simultaneously protecting eelgrass from photodamage. Eelgrass were grown in controlled outdoor aquaria at different aqueous CO_2 concentrations ranging from ~50 to ~2100 µM from May 2013 to October 2014 and examined for differences in leaf optical properties. Even with daily and seasonal variations of temperature and light, CO_2 enrichment consistently increased plant size, leaf thickness and chlorophyll use efficiency, and decreased pigment content and the package effect while maintaining similar light-harvesting efficiency. These acclimation responses suggest that a common photosynthetic sensory function, such as redox regulation, can be manipulated by CO_2 availability, as well as light, and may serve to optimize photosynthetic carbon gain by seagrasses into the Anthropocene.

KEY WORDS: Ocean acidification · Photoprotection · Photosynthesis · Pigments · Seagrass · Temperature · Light

1. INTRODUCTION

The oceans take up nearly one-third of anthropogenic carbon emitted to the atmosphere each year, thereby reducing the rate of climate warming across the globe. This ocean uptake, however, reduces ocean pH and alters fundamental chemical balances in a process called ocean acidification, which is likely to have both positive and negative impacts on marine organisms (Doney et al. 2009). Although terrestrial photosynthesis is predicted to benefit from rising CO_2, at least in the short term, photosynthesis of most marine autotrophs is not limited by CO_2 availability. Photosynthetic rates of ecologically important seagrasses (marine angiosperms) have been shown to benefit significantly from an acidified ocean, and may increase the ability of seagrasses to tolerate a warming ocean climate (Zimmerman et al. 2017, Zimmerman 2021).

Elevated CO_2 environments can produce changes in leaf morphology, stomatal conductance and protein content of terrestrial plants that gradually erode the initial photosynthetic stimulation over time in a process known as photosynthetic acclimation (Li et al. 2013). Nonetheless, leaf size, sugar content and structure of the photosynthetic apparatus of terrestrial plants, including leaf pigment and Rubisco con-

*Corresponding author: celebibillur@gmail.com

tent, appear to be more sensitive to irradiance (i.e. classic photoacclimation) than to CO_2 (Hubbart et al. 2013). However, light can induce stress whenever the photon flux harvested by Photosystem II (PS II) exceeds the electron transport capacity of Photosystem I (PS I) and/or the supply of CO_2 to the Calvin Cycle, which processes that energy into carbohydrates. Such conditions can occur either with increasing irradiance or decreasing photosynthesis in response to other environmental factors, including temperature and CO_2 availability (Demmig-Adams & Adams 1992, Pfannschmidt et al. 2009).

Whenever light energy absorption exceeds the photochemical utilization through photosynthesis, the excess energy must be dissipated through photoprotective mechanisms, such as thermal dissipation and alternative electron flow, to prevent damage to the photosynthetic unit. These flexible and fast-responding photoprotective mechanisms allow plants to cope with fluctuating light environments on time scales of minutes, but prolonged stress can trigger acclimation responses that modify the photosynthetic machinery via changes in gene expression and protein synthesis (Eberhard et al. 2008). Acclimation to high light includes changes in pigment concentration that (1) decrease the optical cross section of PS II, (2) increase the abundance of PS II reaction centers, electron transport carriers and Rubisco that may increase the capacity for light-saturated photosynthesis (Walters 2005) and/or (3) increase the capacity of alternative electron transport reactions in which electron acceptors other than CO_2 become important, such as O_2 leading to photorespiration and/or the Mehler reaction (Niyogi 2000). All of these pathways increase the trans-thylakoid pH gradient within the chloroplast that triggers thermal energy dissipation via the xanthophyll cycle (Demmig-Adams & Adams 1992). For this reason, high light-acclimated plants typically have larger pools of xanthophyll cycle components (i.e. more carotenoids) to dissipate excess photosynthetic energy.

Relative to other marine photoautotrophs, seagrasses have high light requirements for survival (Duarte 1991, Lee et al. 2007) that are partially explained by the metabolic demand of fully functional roots and rhizomes that depend on leaf photosynthesis for reduced carbon (Smith et al. 1988, Zimmerman et al. 1989). However, the relatively weak ability to extract dissolved inorganic carbon from seawater for photosynthesis significantly reduces the ability of these plants to meet their daily metabolic balance (Zimmerman et al. 1997) and limits annual rates of primary productivity and reproductive potential (Palacios & Zimmerman 2007, Zimmerman et al. 2017). The need for long daily periods of light-saturated photosynthesis results in high light requirements for seagrass survival, restricting their distribution to shallow depths and potentially stressful high light environments (Zimmerman et al. 2015, 2017). Seagrasses distributed in these shallow estuarine regions often experience highly dynamic light fields resulting from algae blooms, sediment plumes and tidal variations in water depth and wave action that require a means of photoprotection when excessive light variations become a stress factor, especially under low CO_2 concentrations (Ralph et al. 2002, Buapet et al. 2017, Schubert et al. 2018).

Although seagrass photosynthesis is carbon-limited in the modern ocean, seagrass leaves are nearly as efficient as CO_2-replete algae in terms of light harvesting (Cummings & Zimmerman 2003). This light-harvesting efficiency results from the presence of chloroplasts in the epidermal cell layer, while the inner mesophyll layer contains non-pigmented cells and lacunar spaces that maintain leaf buoyancy and transport O_2 to belowground tissues, and probably facilitate the scattering of light within the leaf that ultimately enhances absorption by the photosynthetic pigments. Adjustments of the primary photosynthetic pigment content in seagrasses allow some capacity for photoacclimation, but the utility of this strategy to compensate for low light availability is limited by the package effect, a result of pigment self-shading in the chloroplast (Cummings & Zimmerman 2003). Accessory carotenoid pigments present in seagrasses serve photoprotection purposes via the xanthophyll cycle (Ralph et al. 2002).

Seagrasses respond to changes in environmental conditions on a variety of temporal and spatial scales (Orth et al. 2006a, Koch et al. 2009). Most recently, seagrasses have been subjected to persistent changes in habitat quality resulting from eutrophication, climate warming and ocean acidification. Eutrophication reduces the light quantity and quality in the water column, and alters sediment biogeochemistry in ways that can limit seagrass growth (Burkholder et al. 2007). Although climate warming is projected to negatively affect seagrasses, particularly those growing near their equatorial distribution limits (Moore & Jarvis 2008, Moore et al. 2012), increasing CO_2 availability resulting from ocean carbonation (ocean acidification) may enhance photosynthetic carbon gain and offset the negative impact of a warming climate (Zimmerman et al. 2017). Zimmerman et al. (2017) demonstrated that CO_2 enrichment of the surrounding seawater quantitatively enhanced the ability of

eelgrass *Zostera marina* L. growing near the southern limit of its geographic distribution on the east coast of North America to tolerate stressful summer water temperatures. In addition to increasing plant survival, enhanced CO_2 availability increased overall plant size, absolute growth rates, accumulation of sugar reserves, vegetative reproduction and flowering. These findings demonstrated that CO_2 availability can moderate metabolic carbon balance and thermal tolerance that affect vegetative survival and reproductive success that ultimately influence the distribution and abundance of eelgrass in nature. Yet, the underlying photoacclimation mechanisms that modulate the observed whole plant responses have not been fully elucidated.

The specific objectives of the present study were to (1) quantify the time-course of photosynthetic acclimation of eelgrass to elevated CO_2 concentrations in the context of ambient variations in light availability and water temperature, and (2) link the changes in light harvesting to the photosynthetic capacity and eventually to eelgrass performance in terms of growth and survival in a changing climate. We hypothesized that the survival, and inevitably, the depth distribution of eelgrass rely on photon use efficiency rather than photon capture efficiency in carbon-limited coastal ecosystems.

2. MATERIALS AND METHODS

2.1. Experimental facility

This experiment was conducted in an outdoor aquatic climate research facility on the shore of Owls Creek at the Virginia Aquarium, Virginia Beach, VA, USA. Owls creek is a small polyhaline estuary located near the southern limit of eelgrass distribution on the Virginia coast just south of the Chesapeake Bay. Salinity fluctuates from 20 to 30 as a function of tidal exchange with the adjacent waters of the Mid-Atlantic Bight and local storm runoff from the small coastal watershed (Sisson et al. 2010). Concentrations of dissolved inorganic nutrients (N ?10 µM, P ?1 µM) are consistently higher than the concentrations required to saturate eelgrass growth based on previous work by Zimmerman et al. (1987).

Natural water from Owls Creek was pumped continuously into a 70 m^3 head tank and gravity-fed into the bottom of 20 fiberglass open-top aquaria (3 m^3 each) at one end of each aquarium. An overflow standpipe at the opposite end of each aquarium provided drainage and kept the water depth at 1 m. The continuous flow system provided a volume turnover rate of 10 d^{-1} in each aquarium. All aquaria were covered with a single layer of neutral density plastic window screen that reduced the incident irradiance by 40% to simulate their natural environment and protect the leaves from photodamage. These screens were removed during February and March 2014 to prevent snow accumulation. All aquaria were bubbled with compressed air delivered through 2 m lengths of Pentair Bio-Weave diffuser hose to enhance turbulent mixing and reduce boundary layer limitation of leaf metabolism.

Beverage-grade CO_2 was injected from a cryogenic storage tank into the diffuser hoses through solenoid valves operated by pH controllers (Eutech Alpha pH 190) poised at a gradient of pH values (4 aquaria at each pH) ranging from ambient (no CO_2 addition, pH ?7.7, $[CO_{2(aq)}]$?50 µM) to pH 6.0 ($[CO_{2(aq)}]$?2100 µM). pH electrodes were calibrated weekly using National Bureau of Standards (NBS) buffers. This system provided excellent separation of the CO_2 treatments throughout the course of the experiment (Zimmerman et al. 2017). The alkalinity of water samples collected periodically from the aquaria was determined by automatic titration (Gieskes & Rogers 1973) and regressed against salinity ($r^2 = 0.86$) to provide a relationship by which alkalinity could be estimated from continuously measured salinity during the experiment. Speciation of dissolved inorganic carbon for each aquarium was calculated from measured values of temperature, pH and salinity/alkalinity using CO2SYS version 1.1 (van Heuven et al. 2011). Although pH values below 7.5 exceed the range of ocean acidification predicted by the Intergovernmental Panel on Climate Change through the end of the 21st century, estuarine systems experience a much wider and more temporally variable range in pH/CO_2 than the open ocean, incorporating much of the experimental range used here (Duarte et al. 2013, Waldbusser & Salisbury 2014, Ruesink et al. 2015). Further, this range provides a useful gradient in CO_2 availability required to determine functional responses (slopes and intercepts) necessary for predicting the future performance of eelgrass in a high CO_2 world.

The aquaria were exposed to daily and seasonal fluctuations of ambient temperature, irradiance and salinity. The temperature was measured in each aquarium using Omega 44005 precision thermistors and custom voltage divider circuits calibrated to a precision of 0.1°C. Sunlight was measured as photosynthetically active radiation (PAR, in air) using a factory-calibrated LI-COR LI190sb plane irradi-

ance sensor (µmol photons m^{-2} s^{-1}) placed 3 m above the aquaria. Salinity was measured using a factory-calibrated SeaBird SBE-37 MicroCAT placed in one of the aquaria. All instrument readings were averaged for 1 min and recorded at 10 min intervals using a National Instruments data acquisition system controlled by custom software written in LabView running under Windows XP. Aquaria, electronic sensors and plants were cleaned weekly to control biofilm accumulation.

The instantaneous in-air PAR measures were integrated to calculate the daily total flux (mol quanta m^{-2} d^{-1}) of screen-corrected surface irradiance. Additionally, the daily periods of irradiance-saturated photosynthesis (H_{sat}), representing the number of hours per day when instantaneous irradiance exceeded the photosynthesis-saturating irradiance ($E_{k\text{-}aquaria}$) values of ~100 and ~400 µmol quanta m^{-2} s^{-1}, were calculated for ambient and CO_2-enriched tanks, respectively. These aquaria E_k values were estimated by applying geometrical correction on precise laboratory measurements of photosynthesis versus irradiance (E_{PAR}) response curves of eelgrass leaves for leaf orientation and the angular distribution of submarine irradiance (Zimmerman 2003, Celebi 2016).

2.2. Source population

Eelgrass shoots, with intact roots and rhizomes, were collected by SCUBA divers using hand tools in May 2013 from a restored eelgrass meadow in South Bay, a coastal lagoon near the southern tip of the DelMarVa (USA) Peninsula (Orth et al. 2006b). Shoots were transferred the same day to the Aquarium Facility in coolers filled with seawater. Approximately 50 vegetative shoots with intact roots and rhizomes were carefully transplanted into plastic trays, filled with sediment collected from Elizabeth River, VA. Five trays were placed into each aquarium randomly, providing ~250 shoots in each aquarium. All aquaria were kept at ambient pH (no CO_2 addition) for 1 mo to permit the recovery of shoots from transplantation shock and to compare transplant performance across the aquaria. CO_2 enrichment of the experimental aquaria was initiated in June 2013 and maintained through October 2014 (18 mo, covering 2 summer growth periods). Additional eelgrass shoots were collected from the same location in April 2014. For each tank, 2 separate trays of these new plants (i.e. 2nd-year transplants) were added next to the acclimated shoots from 2013 (1st-year transplants). These shoots were immediately exposed to CO_2 enrichment.

2.3. Leaf optical properties

For the analysis of leaf optical properties, one 2nd-youngest leaf per aquarium from both 1st-year and 2nd-year transplants were collected monthly. Approximately 5 cm long segments, cut 1 cm above the basal meristem, were cleaned of epiphytes by wiping with a laboratory tissue. Lengths and widths of each segment were measured using a digital caliper. Fresh weights were measured using an analytical balance. Area-specific leaf density was calculated as the ratio of mass to leaf area (mg cm^{-2}, Table 1). Spectral absorbance, $D(\lambda)$, and reflectance, $\rho(\lambda)$, of intact leaf segments within the range 350–750 nm were measured in a Shimadzu UV 2101PC scanning spectrophotometer fitted with an integrating sphere. Photosynthetic leaf absorptances, $A_L(\lambda)$, were corrected by subtracting the non-photosynthetic absorptances at 750 nm, i.e. $A_L(750)$ (Kirk 1994):

$$A_L(\lambda) = [1 - 10^{-D(\lambda)}] - \rho(\lambda) - A_L(750) \quad (1)$$

The photosynthetic absorptances were then used to calculate the leaf-specific photosynthetic absorption coefficients, $a_L(\lambda)$, and the optical cross sections, $a_L^*(\lambda)$:

$$a_L(\lambda) = -\ln [1 - A_L(\lambda)] \quad (2)$$

$$a_L^*(\lambda) = a_L(\lambda) / [\text{Chl } a] \quad (3)$$

Photosynthetic and photoprotective pigments were extracted by homogenizing the leaf segments in a

Table 1. List of abbreviations, their definitions and dimensions. Parenthetic notation '(λ)' denotes wavelength dependence of the variable

Abbreviation	Definition	Units
FW	Fresh weight	mg
H_{sat}	Daily period of irradiance-saturated photosynthesis	h d^{-1}
E_k	Photosynthesis saturating irradiance	µmol quanta m^{-2} s^{-1}
LA	Leaf area	cm^2
Chl *a*	Chlorophyll *a*	µg cm^{-2} or mg g^{-1} FW
Chl *b*	Chlorophyll *b*	µg cm^{-2} or mg g^{-1} FW
TChl	Total chlorophyll	µg cm^{-2} or mg g^{-1} FW
TCar	Total carotenoid	µg cm^{-2} or mg g^{-1} FW
$A_L(\lambda)$	Leaf absorptance	Dimensionless
$D(\lambda)$	Leaf absorbance	Dimensionless
$\rho(\lambda)$	Leaf reflectance	Dimensionless
$a_L(\lambda)$	Leaf-specific absorption coefficient	Dimensionless
$a_L^*(\lambda)$	Optical cross section	m^2 g^{-1} chl *a*
λ	Wavelength	nm

glass tissue grinder with ice-cold 80% acetone. Concentrations of chlorophyll *a* (chl *a*), chl *b* and total carotenoids (TCar) were calculated using the extinction coefficients of Lichtenthaler & Wellburn (1983), except for the first month of sampling. In May 2013, only photosynthetic pigments were extracted using 90% acetone and calculated using the extinction coefficients of Jeffrey & Humphrey (1975).

2.4. Light microscopy observations of leaf cross sections

Freshly collected leaves were cut into 1 cm long segments and wet-mounted to a glass microscope slide using seawater and a thin coverslip. Leaf surfaces were photographed using a digital camera (Olympus DP-70; Olympus DP Controller version 3.2.1.276) coupled to a stereo zoom microscope (Olympus SZX12) with Olympus DF PLAPO 1X PF objective. Leaf cross sections were hand-cut using a razor blade, wet-mounted as above and photographed using a digital camera (Olympus DP-70) coupled to a compound microscope (Olympus BX-50) with an Olympus UPlanFl 10× objective.

2.5. Statistical analysis

Statistical analyses were performed with IBM SPSS Statistics 22, MATLAB R2014b and SigmaPlot 12.5 software packages. Unless otherwise specified, all error estimates represent ±1 SE. Environmental data sampled at high frequency were converted to daily, monthly and total (18 mo) averages to match the sampling frequency of leaf optical properties for cross-correlation analyses. The effects of CO_2 enrichment were analyzed by a repeated measures general linear model (SPSS) with time as the fixed factor (within subjects) and pH as the covariate (between subjects). For the comparison of long-term trends, pH was considered as the main covariate because the levels of this parameter were maintained constant throughout the 18 mo. Aquaria were considered repeated subjects because leaf samples were collected from each aquarium every month. Degrees of freedom were adjusted using the Greenhouse-Geisser Epsilon correction whenever error covariance matrices failed the sphericity assumption. Additionally, the effect of CO_2 on each leaf optical measure within each time level (month) was quantified by linear regression with respect to log [CO_2]. These coefficient estimates for each month (i.e. monthly slopes) were compared using tests of within-subjects contrasts and categorized into 3 groups (high, mean and low) based on the deviation from a mean slope calculated for the overall CO_2 effect.

The simultaneous interacting effects of environmental parameters were analyzed using multiple linear regression models. Leaf properties were regressed against environmental parameters averaged over the 2 wk period preceding the sampling date, as 5 cm leaf segments used for measurements represented on average 3 to 7 d old tissues during warm and cold seasons, respectively (based on monthly growth rates of leaves, sensu Zimmerman et al. 2017). This integrated time analysis accounted for the response time of the leaf properties and determined the relative significance of each environmental factor to drive the observed acclimations. For each leaf optical property, first a general multiple linear regression was performed against all 3 environmental predictors, where data from all pH treatments were aggregated. Additionally, for each pH treatment, separate multiple linear regressions using the backward stepwise method were performed to differentiate the dominant environmental predictors among the different treatments. Within each pH treatment, however, maintaining aquarium pH at constant values resulted in some temporal variation in [CO_2] due to the dependency of CO_2 solubility on temperature, as well as salinity. Therefore, during these treatment-specific multiple linear regression analyses, the collinearity statistics between CO_2 and temperature were evaluated with precaution if the variance inflation factor (VIF) index of collinearity statistics exceeded the threshold value of 2. VIF quantifies the severity of multicollinearity in an ordinary least squares regression analysis.

Finally, the responses of long-term acclimated plants (1st-year transplants) were compared to short-term acclimated plants (2nd-year transplants) using a mixed linear model where the fixed factors were transplantation and time, with pH as a covariate.

3. RESULTS

3.1. Temporal patterns in environmental drivers

Aquarium pH averaged 7.5 during the initial transplant recovery period prior to the onset of CO_2 enrichment in June 2013 (Fig. 1A). From June 2013 to October 2014, the daily average pH values of the enriched treatments were 6.1 ± 0.02, 6.5 ± 0.04, 6.9 ± 0.03 and 7.4 ± 0.04, confirming no

overlap between the treatment levels. The ambient treatments (not enriched with CO_2) experienced natural daily and seasonal variations in pH from the Owls Creek source water driven by local metabolic activity. In summer, the pH in these unmanipulated aquaria ranged daily from a low of 7.3 just before dawn to highs exceeding 8.1 in late afternoon. In winter, the daily pH oscillated between 7.9 and 8.1. The corresponding average concentrations of dissolved aqueous CO_2 [$CO_{2(aq)}$] for the different treatments were 2121 ± 118, 823 ± 80, 371 ± 32, 107 ± 17 and 55 ± 6 µmol CO_2 kg^{-1} seawater (SW) during the enrichment period. Further analysis of CO2SYS variables and additional environmental parameters are presented in Zimmerman et al. (2017).

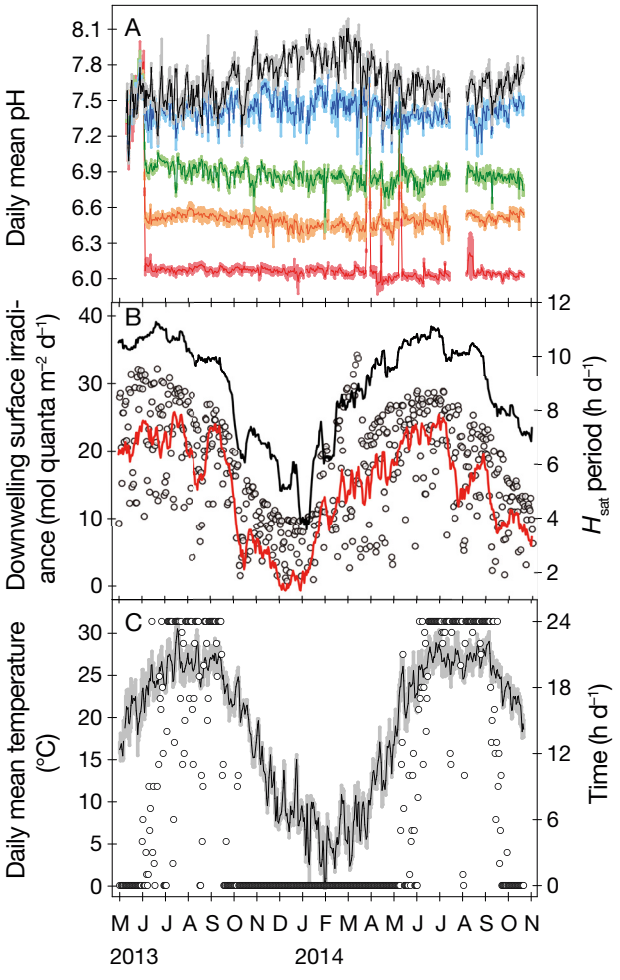

Fig. 1. Temporal patterns in environmental drivers. (A) Average of daily mean pH values of 4 aquaria for each treatment (shading shows SE). The CO_2 enrichment started in June 2013 after the transplant recovery period. Red line: pH 6.1, orange: pH 6.5, green: pH 6.9, blue: pH 7.4, black: pH 7.7 (ambient). (B) Daily surface irradiance (open symbols) scaled according to the left *y*-axis. Solid lines (on the right *y*-axis) show the hours (H_{sat}) each day that the instantaneous light level exceeded the light level required to saturate photosynthesis ($E_{k\text{-}aquaria}$). Black (red) line: $E_{k\text{-}aquaria}$ = 100 (400) µmol quanta m^{-2} s^{-1}. (C) Mean seawater temperature (solid black line) scaled according to the left *y*-axis. Shading around the mean line indicates daily maximum and minimum values. Open symbols (on the right *y*-axis) show the hours each day that the temperature was above the 25°C threshold

Both temperature and downwelling surface irradiance showed seasonal trends as well as daily patterns typical of the mid-Atlantic environment in which the experiment was conducted (Fig. 1). Highest irradiances were observed during June in both years, while the temperature was highest in July and August. Seasonal changes in temperature lagged the light signal by 43 d (r = 0.7). The seasonal amplitude of daily-integrated irradiance varied from 6 to 24 mol quanta m^{-2} d^{-1}, with randomly scattered cloud effects (Fig. 1B). $E_{k\text{-}aquaria}$ for the ambient CO_2 treatment was ~200 µmol quanta m^{-2} s^{-1}, resulting in periods of irradiance-saturated photosynthesis that potentially required photoprotection for at least 4 h d^{-1} and up to 11 h d^{-1} in summer months (Fig. 1B). Because the addition of CO_2 increased the rate of light-limited photosynthesis up to 3-fold and onset of light-saturation up to 400 µmol quanta m^{-2} s^{-1} (McPherson et al. 2015, Celebi 2016), H_{sat} dropped by 27% (i.e. below 8 h) in response to CO_2 availability, thereby reducing the daily need for photoprotection at low pH.

The seawater temperature ranged from 2°C in winter up to 30°C in summer (Fig. 1C). It was consistently lower than 25°C from October 2013 until May 2014, but exceeded the 25°C threshold for the onset of thermal stress in eelgrass more than 1 h d^{-1} for 97 and 124 d in 2013 and 2014, respectively.

3.2. Responses to CO_2 enrichment

Plant size, measured as the 1-sided area of all leaves per shoot, increased linearly with log [CO_2] after 2 mo of growth in the experimental aquaria (Fig. 2A). This CO_2 response, expressed as monthly slopes of plant size vs. log [CO_2], remained consistently positive after July 2013. The largest plant sizes in all treatments were observed in fall 2013 and early summer 2014, which were also the months with highest response to CO_2 enrichment as indicated by 3-fold higher slopes. In addition to more leaf area per shoot, the area-specific leaf density (mg FW cm^{-2}) also increased with log [CO_2] (Table 2). The area-specific leaf density increased in all treatments during the hot months of both years (Fig. 2B) when

the response to CO_2 enrichment was enhanced as well. The rate of increase in area-specific leaf density with available CO_2 ranged from as low as 2 to a maximum of 10 mg FW cm^{-2} $(\log CO_2)^{-1}$, with an overall average of 7 mg FW cm^{-2} $(\log CO_2)^{-1}$ (Fig. 2B). The CO_2 effect was non-significant only in 2 months, one being during the initial acclimation period to the aquarium environment, as expected, and in November 2013 (Fig. 2B). The change in area-specific leaf density, resulting from changing leaf thickness (Fig. 2C), had important consequences when pigment concentrations were normalized either to biomass for interpretation of metabolic acclimation or to area for interpretation of light-harvesting acclimation.

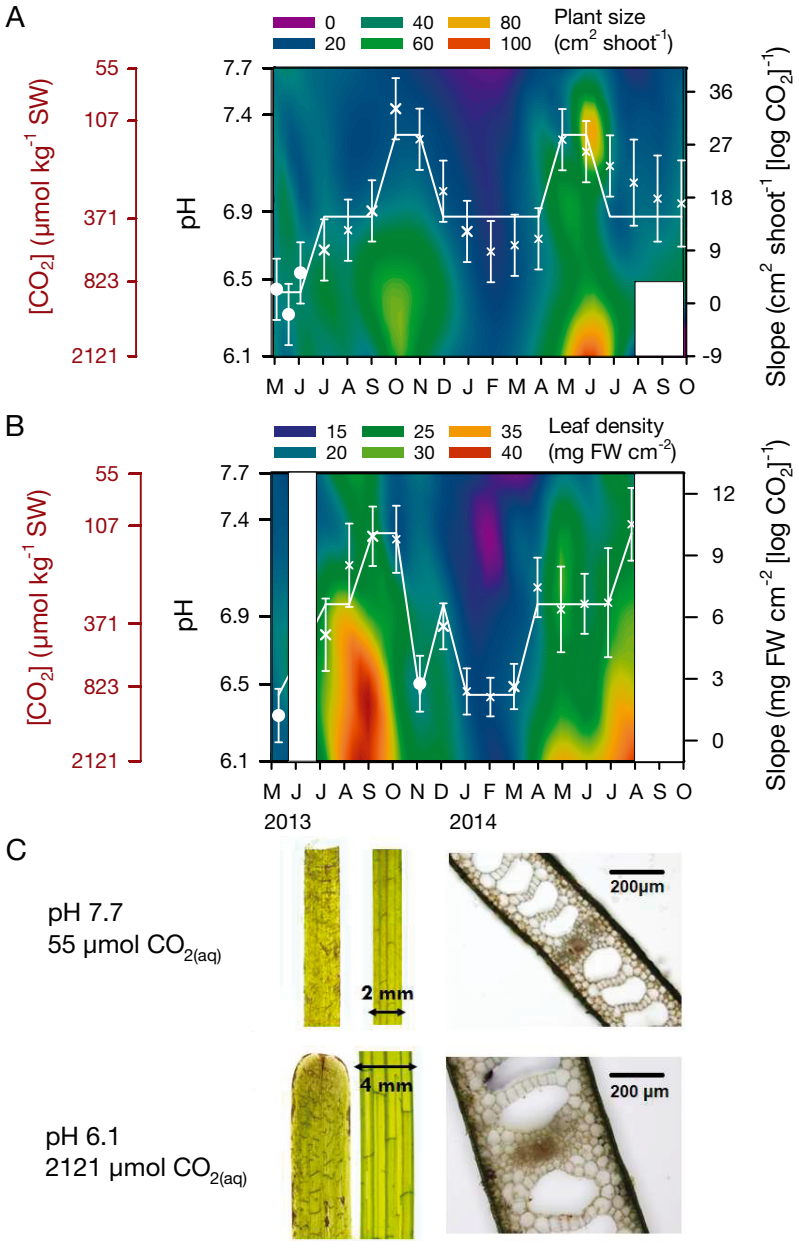

Fig. 2. Heat maps of (A) aboveground plant size and (B) area-specific leaf density, contoured as a function of pH (primary left *y*-axis) over time. Corresponding average $[CO_{2(aq)}]$ values for each treatment are indicated on the secondary *y*-axis. White symbols on each plot represent the slope of the response variable vs. log $[CO_{2(aq)}]$ derived from linear regression analysis (right *y*-axis); statistical significance of the slope is indicated with '×' when regression $p < 0.05$. Error bars represent ±1 SE of the regression slopes. Horizontal lines connect slopes that were statistically identical by within-subject contrasts analysis (calculation details given in Section 2.5). The white fields indicate no data. (C) Micrographs of eelgrass leaves collected from ambient treatment (top) and from high CO_2 treatment (bottom) in September 2013. Left panel shows leaf surfaces, right panel compares horizontal leaf cross sections (i.e. leaf thickness). SW: seawater; FW: fresh weight

All pigment measures, except the chl *a*:*b* ratio, responded significantly to CO_2 enrichment (Table 2). Both area- and biomass-specific pigment concentrations decreased as CO_2 availability increased, indicated by consistently significant negative slopes in pigment content vs. $[CO_2]$ after the acclimation period (Figs. 3 & 4). After 3 mo of CO_2 enrichment, the biomass-specific total chlorophyll (*a* + *b*) content (TChl) of high CO_2 treatments decreased to 35% of ambient treatment, even though all treatments were exposed to the same light environment (Fig. 3A). Although still statistically significant, the effect of CO_2 was less pronounced when TChl was normalized to leaf area (Fig. 3B). On top of the CO_2 response, TChl increased during winter and decreased during summer months in all treatments, resembling classic photoacclimation. As with the CO_2 effect, changes in TChl were more pronounced when normalized to biomass than leaf area. Chl *a*:*b* ratios also responded to seasonal changes in temperature and light but not to CO_2 enrichment (Fig. 3C). Similar to TChl content, TCar content decreased with increasing CO_2, and the decrease was greater when normalized to biomass (Fig. 4A) than area (Fig. 4B). However, the effect of CO_2 on TCar was less than on TChl such that TCar:TChl ratios increased with increasing CO_2, particularly during the winter of 2014 (Fig. 4C).

Table 2. General linear model repeated measures summary table. Abbreviations are defined in Table 1

Measure	Source	Effects df	Error df	*F*	p
FW/LA	pH_{avg}	1	18	292.6	<0.001
	Time	14	252	5.36	<0.001
	Time × pH_{avg}	14	252	3.64	<0.001
Chl *a*/FW	pH_{avg}	1	18	143.0	<0.001
	Time	14	252	2.89	<0.001
	Time × pH_{avg}	14	252	2.57	0.002
Chl *a*/LA	pH_{avg}	1	18	112.5	<0.001
	Time	6	112	3.87	0.001
	Time × pH_{avg}	6	112	3.36	0.004
TChl/FW	pH_{avg}	1	18	144.4	<0.001
	Time	14	252	2.98	<0.001
	Time × pH_{avg}	14	252	2.50	0.002
TChl/LA	pH_{avg}	1	18	114.8	<0.001
	Time	6	106	3.99	0.001
	Time × pH_{avg}	6	106	3.40	0.004
Chl *a*:*b*	pH_{avg}	1	18	1.28	0.273
	Time	5	83	2.67	0.031
	Time × pH_{avg}	5	83	2.85	0.023
TCar/FW	pH_{avg}	1	18	138.7	<0.001
	Time	13	234	1.58	0.093
	Time × pH_{avg}	13	234	1.61	0.083
TCar/LA	pH_{avg}	1	18	83.55	<0.001
	Time	13	234	2.08	0.016
	Time × pH_{avg}	13	234	1.91	0.030
TCar:TChl	pH_{avg}	1	18	15.83	<0.001
	Time	4	75	3.79	0.007
	Time × pH_{avg}	4	75	3.14	0.018
$a_L^*(430)$	pH_{avg}	1	18	123.1	<0.001
	Time	14	252	6.02	<0.001
	Time × pH_{avg}	14	252	4.24	<0.001

The changes in pigment content resulting from CO_2 and light impacted the leaf absorption spectra unequally (Fig. 5A). While absorptances in the green region (i.e. at 550 nm) were more sensitive to CO_2 than season, absorptances within the blue region (430–460 nm), where absorption maxima of chlorophylls co-occur with carotenoids, varied more strongly with seasons, i.e. an almost 20% increase from August 2013 (when highest PAR levels were recorded) to December 2013 (when lowest PAR levels were recorded). The significant differences in chlorophyll content across the CO_2 gradient, combined with differences in leaf absorptances, dramatically impacted $a_L^*(\lambda)$ of intact leaves, which is a measure of chlorophyll use efficiency (Fig. 5B). Because the highest variability in the spectral $a_L^*(\lambda)$ across treatments was observed within the Soret region (400–450 nm) primarily responsible for driving photosynthesis, $a_L^*(430)$ was chosen to represent the response of $a_L^*(\lambda)$ to CO_2 enrichment through time (Fig. 5C). In all seasons, after the initial acclimation period, CO_2 enrichment increased $a_L^*(430)$ significantly, implying increased chlorophyll use efficiency due to a reduced package effect when photosynthesis was stimulated by CO_2 availability.

Increasing CO_2 caused a reduction in TChl content, but it also increased the thickness of the unpigmented mesophyll layer of the leaves. Thus, the biomass-specific TChl content (i.e. slope of the TChl vs. leaf density) decreased as CO_2 increased/pH decreased (Fig. 6A). The 5-fold increase in area-specific leaf density produced a barely perceptible 8% decrease in the absorptance at 677 nm (Fig. 6B) that was unaffected by the CO_2 treatments. The optical cross section $a_L^*(\lambda)$, a measure of TChl use efficiency, was not significantly affected by area-specific leaf density (i.e. leaf thickness) but increased consistently with CO_2 treatment (Fig. 6C, Table 3). As a result, $a_L^*(\lambda)$ decreased exponentially with TChl in a manner that was consistent across all treatments, a result of pigment self-shading (Fig. 7A). This package effect causes the relationship between leaf absorption and TChl to be non-linear (Fig. 7B–D). Strong absorption bands in the blue (440 nm) and red (677 nm) regions caused self-shading to occur at lower pigment concentrations (2.78 and 5.26 µg cm^{-2}, respectively) than in the green region (550 nm) which required 14.3 µg chl cm^{-2} to reach optical saturation. Whereas the chlorophyll concentrations of ambient treatments were higher than these threshold values throughout the experiment, self-shading of TChl decreased as CO_2 increased (Fig. 7B).

3.3. Seasonal responses induced by light and temperature

Area-specific leaf density increased with CO_2 but more significantly with temperature (indicated by higher standardized coefficients) (Table 3). Within each CO_2 treatment, temperature was the most significant environmental predictor of area-specific leaf density, whereas light had no significant effect (Fig. 8A, Table 4). Area-specific TChl content showed a stronger negative relationship with CO_2 than with light and a positive relationship with temperature (Fig. 8B, Table 3). The response of chlorophyll content to temperature was reversed when normalized to biomass (Table 3), most likely because of increasing leaf thickness (by non-photosynthetic tissues) during summer.

Analysis of CO_2 treatments individually highlighted that the regulating environmental factor of area-specific chlorophyll content depended on the CO_2

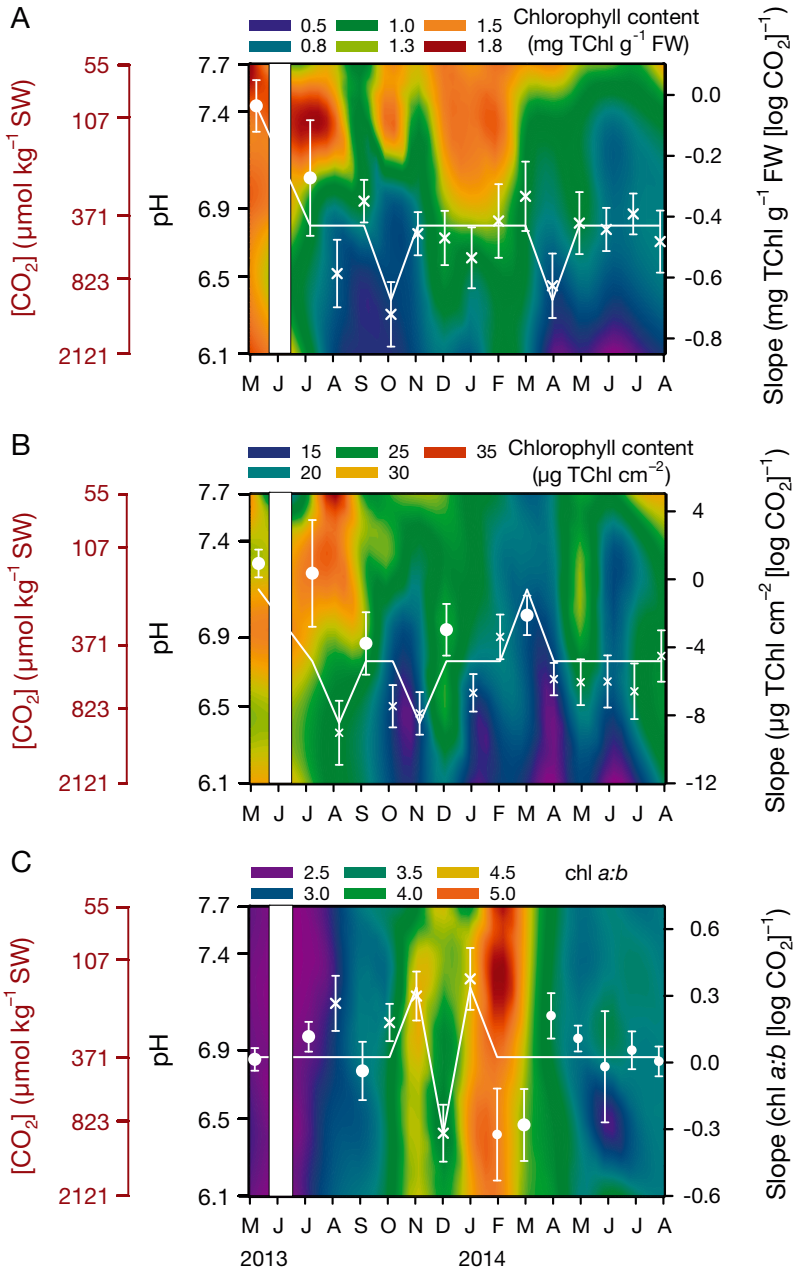

Fig. 3. Heat maps of total chlorophyll (*a+b*) (TChl) (A) per biomass and (B) per leaf area and (C) their ratios, contoured as a function of pH (primary left *y*-axis) over time. Other details as in Fig. 2A,B

environment (Table 4). Chlorophyll content of ambient plants responded positively to increasing temperature and negatively to increasing light, whereas the natural seasonal cycle of [CO_2] had no significant impact (Fig. 8B). TChl content of eelgrass grown under CO_2 stimulation, however, did not change significantly with changing light or temperature (represented by the red horizontal plane in Fig. 8B) but responded to the seasonal CO_2 variability in their high CO_2 environment (as indicated by the statistically significant beta values for the daily average log[CO_2] parameter in Table 4). Like TChl, carotenoid content was most responsive to [CO_2] (Table 3). Increasing light played a secondary role in decreasing carotenoid content. Temperature had a significant effect on carotenoid content only in the low CO_2 treatments (Fig. 8C, Table 4).

CO_2 enrichment did not change the chl *a:b* ratio significantly (Table 3). The ratio decreased profoundly with increasing temperature but not with light (Fig. 9A). Chl use efficiency, as measured by $a_L^*(\lambda)$, increased with CO_2 but decreased with temperature, indicating a strong package effect in the low CO_2, high temperature environment of summer (Fig. 9B). Leaf absorptance (at 677 nm), which was negatively correlated with area-specific density (i.e. leaf thickness) (Table 3), decreased in response to both increasing light and temperature. Despite the strong negative effect on pigment concentration, CO_2 treatment was the least significant predictor of leaf absorptance (Fig. 9C).

3.4. Response time of leaf properties to CO_2 enrichment

CO_2 enrichment of the second set of eelgrass transplants, freshly collected from the same field location in the spring of 2014 and grown together with eelgrass plants exposed to CO_2 enrichment since spring of 2013, showed the differences in response time of leaf properties to [CO_2]. It took nearly 4 mo for specific growth rate, area-specific chlorophyll content, chl *a:b* ratio and $a_L^*(430)$ of the 2014 transplants to converge with those of the 2013 transplants in all treatments (Table 5, as indicated by the non-significant transplantation × pH_{avg} interaction measure). However, the area-specific leaf density, plant size and area-specific carotenoid content of 2014 transplants did not converge with the 2013 transplants during the course of this experiment (Fig. 10), meaning that these properties exhibit a

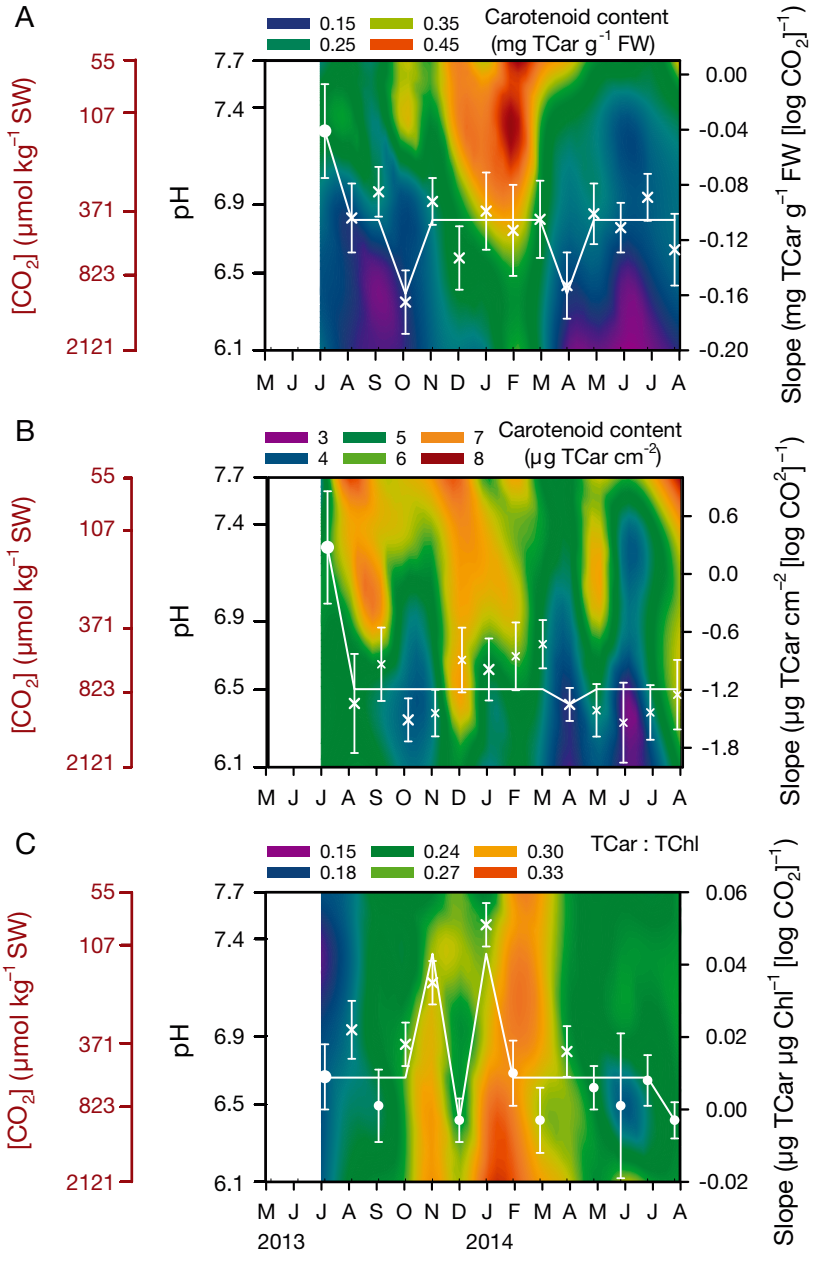

Fig. 4. Heat maps of total carotenoids (TCar) (A) per biomass and (B) per leaf area, and (C) their ratios to photosynthetic pigments as a function of pH (primary left *y*-axis) over time. Other details as in Fig. 2A,B

longer response time to CO_2 enrichment. Therefore, the minimal experimental duration required to detect the impact of CO_2 enrichment depends on the response variable being monitored.

4. DISCUSSION

CO_2 enrichment increased both biomass yield (i.e. biomass per leaf area) and the size of eelgrass plants (i.e. leaf area per shoot), likely because of increased photosynthetic yield and carbohydrate assimilation (Zimmerman et al. 2017). However, the pigment content of eelgrass leaves decreased under CO_2 stimulation even though the light environment was identical across all treatments. Although pigment adjustments are typically interpreted as a response to light availability (Demmig-Adams & Adams 1992, Ralph et al. 2002, Dattolo et al. 2014), the down-regulation of pigment content in eelgrass leaves in response to increased [CO_2] suggested that availability of CO_2, the primary substrate for the dark reactions of photosynthesis, can also play a critical role in regulating the light-harvesting complex (Backhausen & Scheibe 1999, Pfannschmidt 2003, Hanke et al. 2009, Hüner et al. 2012). Redox feedback mechanisms are under the control of the oxidation state of plastoquinone in the thylakoid membrane that depends on the continuity of the electron transport under various limiting conditions (Pfannschmidt 2003, Pfannschmidt & Yang 2012). Thus, in addition to energy capture, the photosynthetic machinery performs an important sensory function which further explains the interdependent regulation of pigment composition and optical properties of eelgrass leaves by CO_2, temperature and light.

Physiological optimization of photosynthesis requires a balance between the photochemistry (photon energy capture, electron transport) and biochemistry that drive photosynthesis (Pfannschmidt & Yang 2012). The enzymatic reactions of Rubisco, i.e. photosynthesis and photorespiration, are both sensitive to increasing temperature but antagonistically respond to increasing CO_2. Relative to photosynthesis, however, recycling of CO_2 and Calvin-Benson Cycle intermediates through photorespiration increases the energy requirement from the light reactions that can be generated via absorbing more photons (Jones et al. 2012). The requirement of more photon absorption due to increasing photorespiration with increasing temperature might explain the

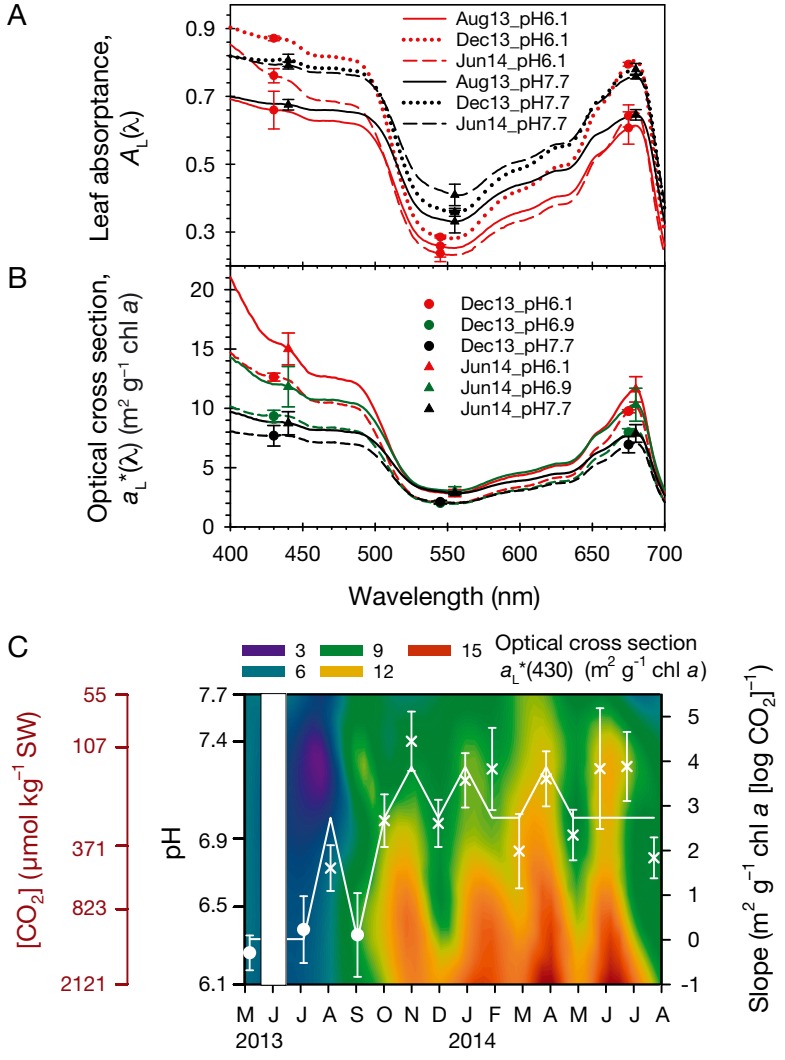

Fig. 5. (A) Spectral average leaf absorptance and (B) average optical cross section for different CO_2 treatments during August 2013 (highest photosynthetically active radiation [PAR] level, [µmol photons m^{-2} s^{-1}]), June 2014 (highest daily total PAR, [mol photons m^{-2} d^{-1}]) and December 2014 (lowest PAR and lowest daily total PAR). Error bars represent ±1 SE. (C) Heat map of optical cross section (analyzed only for a single wavelength, at 430 nm) as a function of pH (primary left *y*-axis) throughout time. Corresponding average [$CO_{2(aq)}$] values for each treatment are indicated on the secondary left *y*-axis. White field indicates no data

increasing area-specific chlorophyll content of eelgrass leaves with increasing temperature in our carbon-limited treatments. This hypothesis coincided with decreasing quantum efficiency of eelgrass leaves under photorespiratory conditions (Celebi 2016). In contrast, growth in a high CO_2 environment increases photosynthetic rates and reduces the need for alternative electron pathways, such as photorespiration, to provide photoprotection, which would explain the negative relationship between chlorophyll content and CO_2 availability in eelgrass revealed by this experiment.

Similarly, increasing photosynthetic capacity of plants acclimated to a high CO_2 environment, as observed by Celebi (2016), could decrease the need for photoprotection by carotenoids. De-epoxidation of carotenoids in the xanthophyll cycle with increasing light is fast (minutes), while epoxidation recovery when light decreases is slow (hours), especially under additional stress (Demmig-Adams & Adams 1996). Therefore, a larger pool of carotenoids may allow CO_2-limited eelgrass to exploit the non-photochemical quenching dissipation pathway more effectively to reduce photo-oxidative damage, given that these plants are exposed to photosynthetic saturating light levels more than 9 h d^{-1} during summer in addition to heat stress due to carbon limitation of photosynthesis. Supporting evidence for this argument was reported by Celebi (2016), who found that CO_2-limited eelgrass regulated NPQ more dynamically in response to increasing light and CO_2.

Reduced pigment content in response to CO_2 enrichment increased the chlorophyll use efficiency and optical cross section, but reduced the leaf absorptances, more in green A(550) than red A(680). These spectral signatures of CO_2 acclimation may need to be incorporated into remote sensing algorithms for productivity estimation. This reduction in photon capturing efficiency in the red seemed to be correlated more with the increasing area-specific leaf density. Assuming the volumetric leaf density was unchanged (a requirement for maintenance of submerged leaf buoyancy), the increases in area-specific leaf density reported here likely resulted from increasing leaf thickness. Microphotographs of leaf cross sections also revealed the differences in leaf thickness between CO_2-enriched and ambient treatments, coinciding with the maximal increase of area-specific density as a function of [CO_2]. Observations of varying leaf thickness in response to light requirements have been reported in other studies (Enríquez et al. 1995, Schubert et al. 2018). A comparative study among various terrestrial

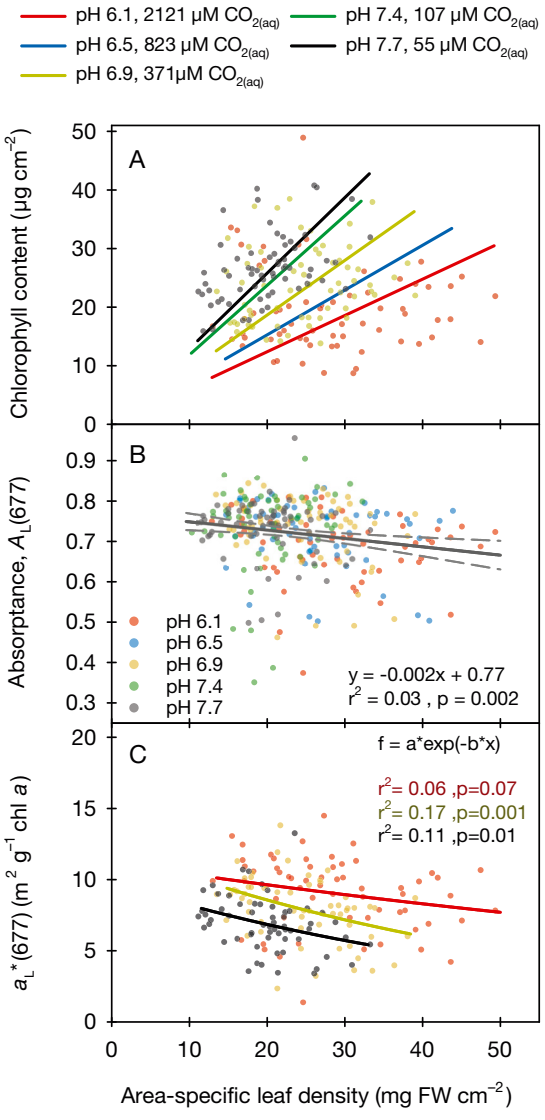

Fig. 6. Effects of CO_2 enrichment on (A) chlorophyll content, (B) leaf absorptance at 677 nm and (C) optical cross section at 677 nm as a function of the area-specific leaf density. Color codes, identical in all panels, represent different CO_2 treatments. For graphical clarity, only data points from 3 CO_2 treatments were plotted in (A) and (C). Solid lines represent linear regression analysis in (A) and (B) and nonlinear regression analysis in (C)

and aquatic photosynthetic organisms by Agustí et al. (1994) identified that thick aquatic plants minimize absorption per unit weight. However, increased thickness of the non-pigmented mesophyll and lacunar space would not alter the light capture efficiency per unit chlorophyll, since photosynthetic pigments of seagrasses are found only in the epidermal layers. Although restricting photosynthetic pigments to the epidermis in aquatic plants, such as in seagrasses, may be required for gas exchange (Zimmerman 2006), it likely enhances the package effect relative to terrestrial plant leaves in which pigments are distributed through several vertical layers of mesophyll cells. This 2-dimensional anatomical constraint causes light-harvesting acclimation to operate at the areal scale for aquatic plant leaves while metabolic acclimation, especially respiration, is expressed in terms of biomass (Vogelman et al. 1996, Walters 2005). Consequently, normalizing to area proved to better illustrate light-harvesting acclimation in eelgrass because normalization of changes in pigment content to biomass overestimated the full extent of changes in light-harvesting capacities.

Even with shade screens attached, the shallow outdoor aquaria used in this experiment created a high light environment for the eelgrass in which photo-

Table 3. Summary of linear regression comparisons with their relative importance coefficients. *significant at $p < 0.005$. PAR: photosynthetically active radiation; other abbreviations are defined in Table 1

Standardized coefficients (significance)	Multiple linear regression (3 predictors)			(a) Simple linear regression (1 predictor) (b) Multiple linear regression (2 predictors)		
Dependent variable:	Daily average log[CO_2]	Daily average temp	Daily total PAR		FW per LA (mg cm^{-2})	TChl per LA (µg cm^{-2})
FW per LA (mg cm^{-2})	0.456*	0.731*	−0.103 (p = 0.039)			pH dependent
TChl per LA (µg cm^{-2})	−0.467*	0.397*	−0.184*			
TChl per FW (mg g^{-1})	−0.591*	−0.329*	−0.005 (p = 0.929)			
TCar per LA (µg cm^{-2})	−0.487*	0.148 (p = 0.024)	−0.342*			
Chl *a*:*b*	0.035 (p = 0.332)	−0.697*	−0.154*	(a)	−0.418*	
TCar:TChl	0.180*	−0.544*	−0.119 (p = 0.044)		−0.325*	
A(550) (%)	−0.517*	0.146 (p = 0.029)	−0.170 (p = 0.011)	(b)	−0.206*	0.479*
A(677) (%)	−0.151*	−0.236*	−0.209*		−0.173*	−0.099 (p = 0.084)
a_L* (430) (m^2 g^{-1} chl *a*)	0.448*	−0.417*	0.124 (p = 0.052)	−0.018 (p = 0.565)		−0.834*
a_L* (677) (m^2 g^{-1} chl *a*)	0.351*	−0.443*	0.123 (p = 0.065)	−0.086 (p = 0.014)		−0.795*

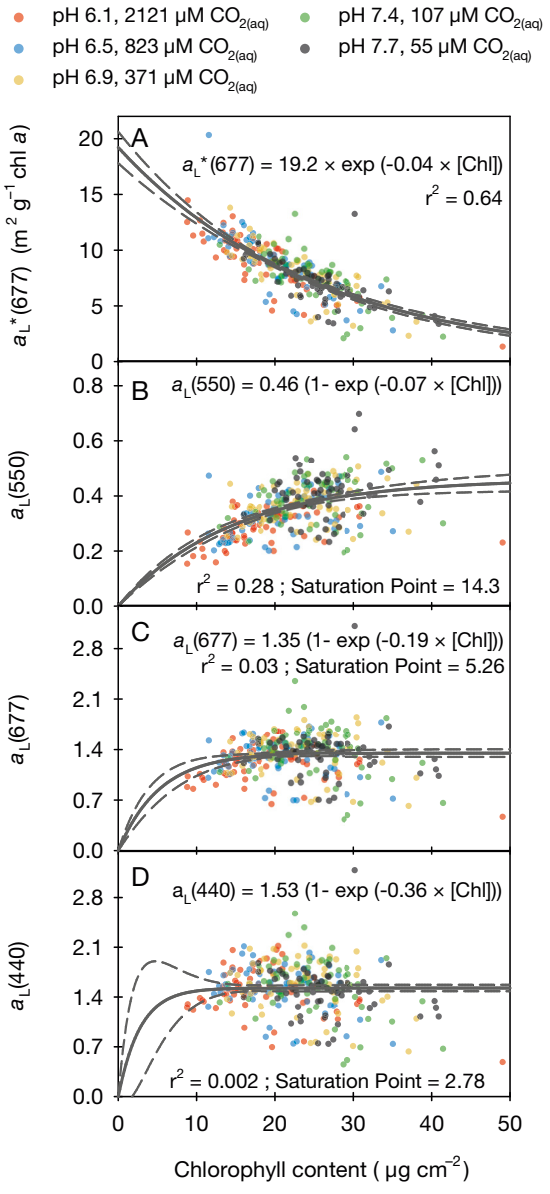

Fig. 7. (A) Optical cross section, $a_L^*(\lambda)$, at 677 nm, and leaf-specific absorption coefficients, $a_L(\lambda)$, at (B) 550, (C) 677 and (D) 440 nm as a function of photosynthetic pigment content for all leaves collected throughout the experiment across CO_2 treatments (represented by different colors). Solid lines represent nonlinear regression analysis with 95% confidence intervals (dashed lines)

synthesis was light-saturated for at least 4 h in the winter and 11 h in the summer. However, in the absence of CO_2 stimulation, the high light environment was insufficient to maximize growth and to protect eelgrass from heat stress (Zimmerman et al. 2017), even though higher photosynthetic pigment concentrations maximized the light-harvesting capacity. Despite reduced light-harvesting capacity,

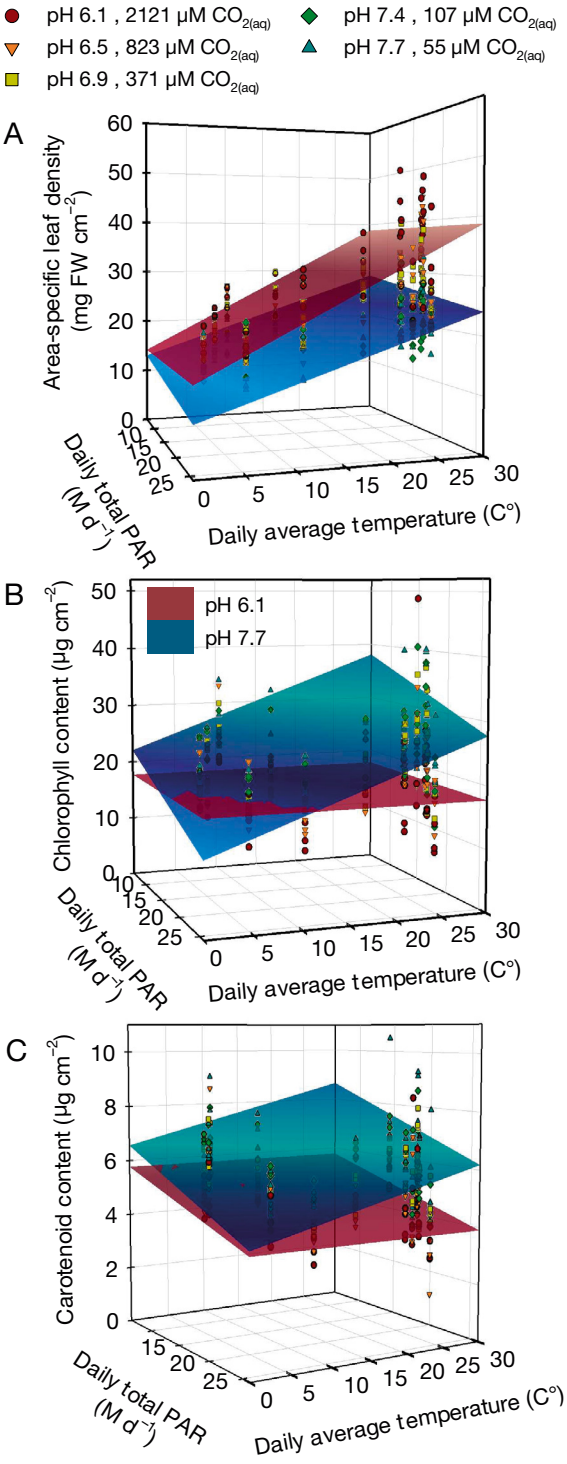

Fig. 8. Interactive effects of temperature and daily total irradiance (photosynthetically active radiation, PAR) on: (A) area-specific leaf density, (B) chlorophyll content and (C) carotenoid content. All data from time-series are shown with symbols and are color-coded for specific CO_2 treatments. Three-dimensional planes were modeled by multiple linear regression analysis. Orientation of axes is arranged to enhance visual clarity. Red plane: response of pH 6.1 treatment, blue plane: response of pH 7.7 (ambient) treatment

Table 4. Multiple linear regression model results for effects of environmental parameters on leaf optical properties specific for each pH treatment. (exc.: as defined by the backward stepwise method, parameters were excluded from the model if the significance level of their *F*-values was >0.10). VIF: variance inflation factor; PAR: photosynthetically active radiation; other abbreviations are defined in Table 1

Backward stepwise linear regression		pH 6.1		pH 6.5		pH 6.9		pH 7.4		pH 7.7	
		Beta	p	Beta	p	Beta	p	Beta	p	Beta	p
FW per LA ($mg\ cm^{-2}$)	Daily average log[CO_2]	exc.		exc.		exc.		0.311	0.026	exc.	
	Daily total PAR	exc.		exc.		exc.		exc.		−0.239	0.068
	Daily average temp	0.764	<0.001	0.741	<0.001	0.743	<0.001	0.879	<0.001	0.832	<0.001
TChl per LA ($\mu g\ chl\ cm^{-2}$)	Daily average log[CO_2]	−0.375	0.004	−0.351	0.008	−0.475	<0.001	exc.		exc.	
	Daily total PAR	exc.		exc.		exc.		exc.		−0.489	0.001
	Daily average temp	exc.		exc.		exc.		0.378	0.004	0.796	<0.001
TCar per LA ($\mu g\ car\ cm^{-2}$)	Daily average log[CO_2]	−0.356	0.020	exc.		exc.		0.497	0.049[a]	exc.	
	Daily total PAR	−0.450	0.004	−0.293	0.028	exc.		−0.822	0.001[a]	−0.509	0.003
	Daily average temp	exc.		exc.		exc.		0.765	0.021[a]	0.449	0.008
Chl *a*:*b*	Daily average log[CO_2]	0.581	<0.001	exc.		0.346	0.021[a]	exc.		−0.239	0.022
	Daily total PAR	−0.291	0.006	−0.251	0.009	−0.225	0.029[a]	exc.		exc.	
	Daily average temp	exc.		−0.672	<0.001	−0.358	0.031[a]	−0.814	<0.001	−0.652	<0.001
A(677) (%)	Daily average log[CO_2]	exc.		exc.		0.523	<0.001	0.225	0.086	−0.575	<0.001
	Daily total PAR	−0.314	0.045	exc.		exc.		−0.264	0.045	exc.	
	Daily average temp	−0.265	0.089	−0.354	0.007	exc.		exc.		exc.	
$a_L^*(430)$ ($m^2\ g^{-1}$ chl *a*)	Daily average log[CO_2]	0.562	<0.001	0.416	0.001	0.610	<0.001	exc.		−0.485	0.003
	Daily total PAR	exc.		exc.		exc.		exc.		0.603	<0.001
	Daily average temp	exc.		exc.		exc.		−0.304	0.023	−0.514	0.001

[a] collinearity statistics VIF > 2.0

eelgrass grown under high CO_2 conditions was more efficient at converting the harvested solar energy into biochemically fixed carbon that resulted in increased biomass accumulation per leaf area and plant size, thus allowing the plants to store enough carbon resources to support higher respiration under heat stress (Zimmerman et al. 2017). Therefore, the survival, and inevitably the depth distribution, of eelgrass rely on photon use efficiency rather than photon capture efficiency in carbon-limited coastal ecosystems. Any environmental signal causing perturbation in photosynthesis thus will trigger acclimation, and a regulatory strategy based on photosynthesis itself will allow the plant to compensate various stress conditions with similar mechanisms (Anderson et al. 1995). Such a strategy would also explain why the elevated CO_2 response of leaf optical properties resembled high light response. The optical cross section $a_L^*(\lambda)$, accepted as a measure of photoacclimation in changing light environments (Cummings & Zimmerman 2003), responded to increasing CO_2 as if the light was increased, meaning that the underlying mechanisms of this acclimation are regulated by a common photosynthetic control mechanism, such as the redox state in the chloroplast.

Although the outdoor design of this experiment provided important natural variability in a number of environmental drivers that is often absent from laboratory experiments (Andersson et al. 2015), the seasonal variations in light and temperature were not fully independent of each other. However, the 43 d lag between light and temperature, considering the sampled leaf tissues were less than 2 wk old, and the removal of shade during February and March 2014 probably reduced the VIF index of collinearity statistics in multiple linear regression analyses. The low VIF index in this study assured the multiple linear regression models with CO_2, temperature and light as predictors to be a significant explanatory fit. The wide CO_2 range across the treatments under a wide range of light and temperature environments quantitatively estimated the general linear response of leaves to the long-term trend of ocean carbonation. Furthermore, the treatment-specific regression analyses indicated that the relative importance of environmental parameters (temperature, CO_2 and light) controlling the leaf properties differed under various CO_2 scenarios, thereby highlighting the thresholds for different acclimation strategies.

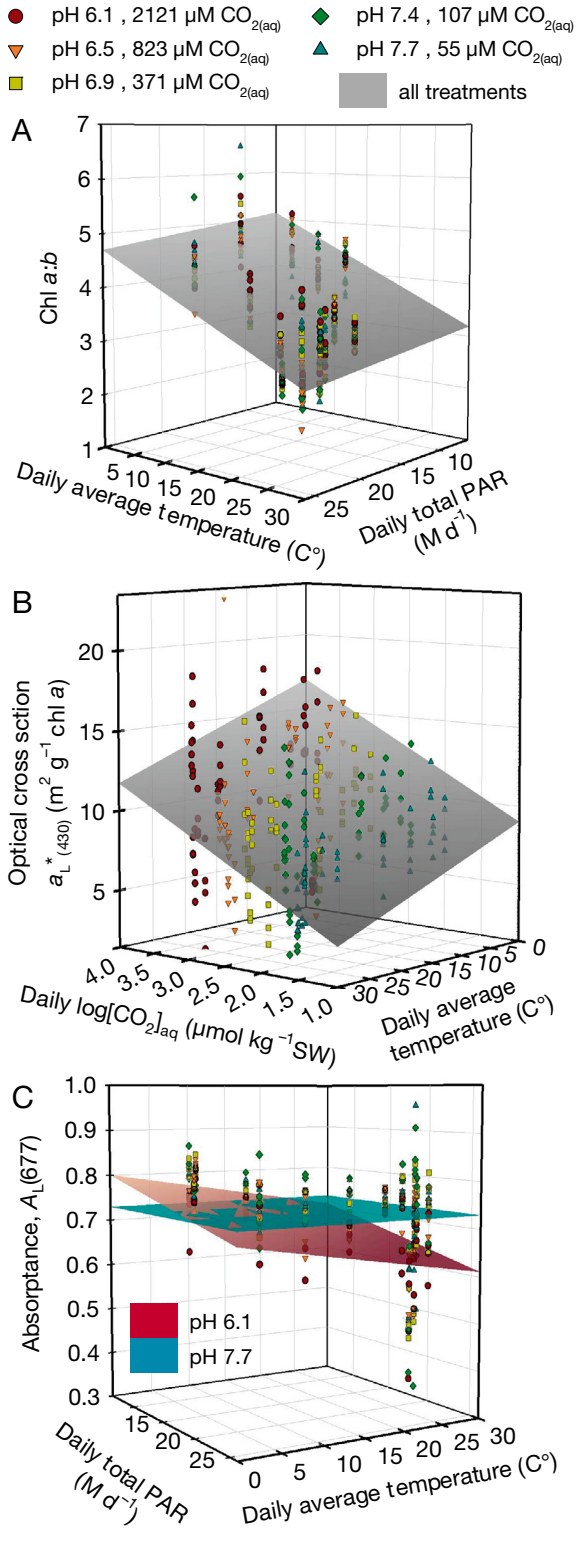

Fig. 9. Interactive effects of CO_2, temperature and daily total irradiance (photosynthetically active radiation, PAR) on: (A) chlorophyll *a:b* ratio, (B) optical cross section and (C) absorptance at 677 nm. Gray plane: response of all treatments combined, red plane: response of pH 6.1 treatment, blue plane: response of pH 7.7 (ambient) treatment. Other details as in Fig. 8

Photosynthetic acclimation is a dynamic process operating at various timescales. This study lasted for 18 mo, allowing the annual rhythm of eelgrass performance to be examined under a gradient of CO_2 concentrations superimposed upon natural fluctuations of environmental parameters. Acclimation of area-specific leaf density and plant size of eelgrass had a long response time, similar to acclimation of the root:shoot ratio (Zimmerman et al. 2017). Long-term developmental processes responding to changes in growth conditions, such as changing leaf anatomy and root:shoot ratios, have been observed to take weeks to months to occur (Longstaff & Dennison 1999, Walters 2005, Lee et al. 2007). In contrast, adjustments of photosynthetic machinery operate on much shorter timescales (Demmig-Adams & Adams 1992), as evidenced by the agreement of photosynthetic pigment composition of transplants from both years when exposed to the same environmental conditions regardless of their growth history. It has been suggested that previous growth history and the natural limits of the physiological tolerance of a species may play a role in acclimation ability and its detection (Yin & Johnson 2000, Walters 2005). Short-term CO_2 enrichment experiments often conclude minimal/varying effects on seagrass physiology and fail to assess the longer-term capacity for acclimation (Cox et al. 2016, Ow et al. 2016, Repolho et al. 2017, Collier et al. 2018, Schneider et al. 2018). In this study, the similarities and differences of multiple parameters among the different transplants (i.e. 1st-year vs. 2nd-year plants) under the same conditions emphasize the importance of timescale in studies of CO_2 acclimation, and justify the need for long-term experiments to understand the impact of climate change on acclimation mechanisms, an important consideration for the design of future Free Ocean CO_2 Experiments (Gattuso et al. 2014, Andersson et al. 2015, Stark et al. 2019).

To conclude, this experiment demonstrated that the composition of light-harvesting and photoprotective pigments in eelgrass responds more dramatically to the availability of CO_2 than to seasonal variations in light or temperature. Increasing chlorophyll use efficiency and the decreasing role of photoprotection in high CO_2 acclimated plants indicated that utilization of absorbed light energy efficiently for photosynthetic carbon assimilation might be the key for long-term regulation of leaf morphology. Further experiments to address the rates of photochemical pathways in such acclimated plants with respect to changes in CO_2, light and temperature would help to understand the rate-limiting physio-

Table 5. Mixed linear model results for comparison of leaf optical properties between long- and short-term acclimated eelgrass leaves. Abbreviations as in Table 1. *significant at $p < 0.05$

Measure Source	TChl per LA (µg cm^{-2}) p	TCar per LA (µg cm^{-2}) p	Chl *a:b* p	FW per LA (mg cm^{-2}) p	a_L*(430) (m^2 g^{-1} chl *a*) p	Plant size (cm^2 shoot^{-1}) p	Specific growth rate (d^{-1}) p
Intercept	0.164	0.824	<0.001*	<0.001*	<0.001*	<0.001*	0.001*
Transplantation	0.074	0.003*	0.153	<0.001*	0.160	<0.001*	0.348
Time	0.077	0.254	0.608	0.278	0.004*	0.855	0.295
pH_{avg}	<0.001*	<0.001*	0.121	<0.001*	<0.001*	0.001*	0.740
Transplantation × Time	0.801	0.860	0.678	0.557	0.854	0.759	0.306
Transplantation × pH_{avg}	0.128	0.004*	0.147	<0.001*	0.234	0.001*	0.326
Time × pH_{avg}	0.325	0.731	0.707	0.292	0.017*	0.861	0.414
Transplantation × Time × pH_{avg}	0.793	0.943	0.760	0.749	0.843	0.843	0.290

logical processes in redox regulation that trigger acclimation responses. Even so, being able to persist for almost 100 million years in highly dynamic coastal systems combined with long-term climate trends highlights both the plasticity and the strong acclimation capacity of seagrass populations. In addition to understanding the underlying mechanisms for their competitive survival in a dynamic system, this study quantified the long-term regulation of light harvesting in response to ocean carbonation to predict the extent of seagrasses in future climatic conditions.

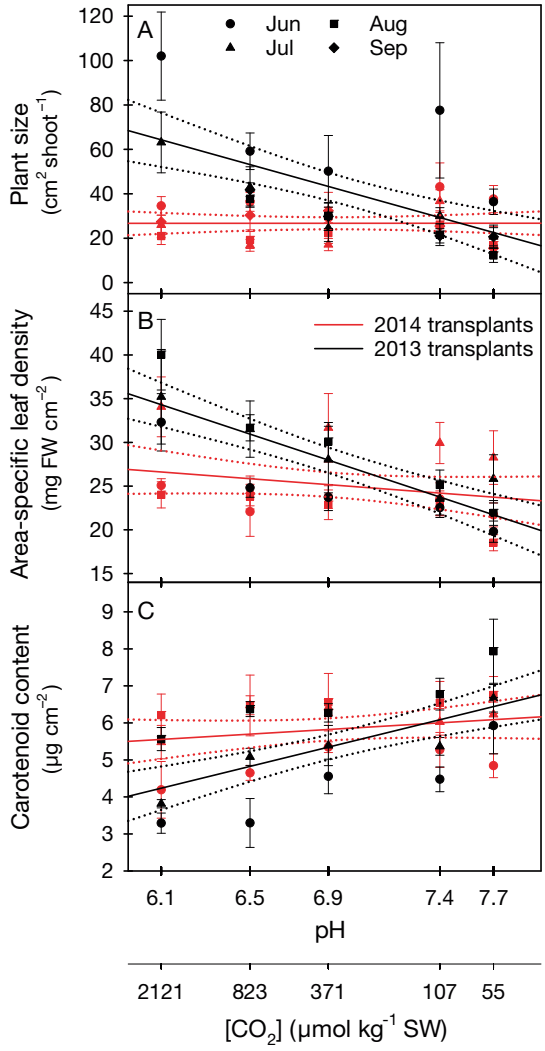

Fig. 10. Validation of acclimation response time to CO_2 enrichment of (A) aboveground plant size, (B) area-specific leaf density and (C) photoprotective pigments via comparison of 1st-year (2013) and 2nd-year (2014) transplants during summer 2014. Symbols represent months, colors represent transplant years. Solid lines represent linear regression analysis with 95% confidence intervals (dashed lines)

Acknowledgements. Thanks to W. M. Swingle and the staff of the Virginia Aquarium & Marine Science Center for maintenance of the experimental facility, and to D. Ruble, M. Jinuntuya, C. Zayas-Santiago, T. Cedeno and M. Smith for assistance with experimental procedures and maintenance of the experimental plants. Thanks to C. M. Powell (ODU) for assistance with LabView programming and integration of the CTD into the environmental monitoring system and to S. Bourgeois and C. Jourdant (Virginia Aquarium) for construction and operational maintenance of the water intake system during the experiment. Thanks to Prof. F. Dobbs for helping with micrography acquisition. Financial support for this research was provided by the National Science Foundation (Award OCE-1061823 to R.C.Z. and V.J.H.), Virginia Sea Grant/NOAA (Award NA14OAR4170093 to R.C.Z. and B.C.E.) and the Department of Ocean, Earth & Atmospheric Sciences, Old Dominion University (to B.C.E.).

LITERATURE CITED

Agustí S, Enríquez S, Frost-Christensen H, Sand-Jensen K, Duarte CM (1994) Light harvesting among photosynthetic organisms. Funct Ecol 8:273–279

Anderson JM, Chow WS, Park YI (1995) The grand design of photosynthesis: acclimation of the photosynthetic apparatus to environmental cues. Photosynth Res 46: 129–139

Andersson AJ, Kline DI, Edmunds PJ, Archer SD and others (2015) Understanding ocean acidification impacts on organismal to ecological scales. Oceanography 28:16–27

Backhausen JE, Scheibe R (1999) Adaptation of tobacco plants to elevated CO_2: influence of leaf age on changes in physiology, redox states and NADP-malate dehydrogenase activity. J Exp Bot 50:665–675

Buapet P, Makkliang F, Thammakhet-Buranachai C (2017) Photosynthetic activity and photoprotection in green and red leaves of the seagrasses, *Halophila ovalis* and *Cymodocea rotundata*: implications for the photoprotective role of anthocyanin. Mar Biol 164:182

Burkholder JM, Tomasko DA, Touchette BW (2007) Seagrasses and eutrophication. J Exp Mar Biol Ecol 350: 46–72

Celebi B (2016) Potential impacts of climate change on photochemistry of *Zostera marina* L. PhD thesis, Old Dominion University, Norfolk, VA

Collier CJ, Langlois L, Ow Y, Johansson C and others (2018) Losing a winner: thermal stress and local pressures outweigh the positive effects of ocean acidification for tropical seagrasses. New Phytol 219:1005–1017

Cox TE, Gazeau F, Alliouane S, Hendriks IE, Mahacek P, Le Fur A, Gattuso JP (2016) Effects of *in situ* CO_2 enrichment on structural characteristics, photosynthesis, and growth of the Mediterranean seagrass *Posidonia oceanica*. Biogeosciences 13:2179–2194

Cummings ME, Zimmerman RC (2003) Light harvesting and the package effect in the seagrasses *Thalassia testudinum* Banks ex König and *Zostera marina* L.: optical constraints on photoacclimation. Aquat Bot 75:261–274

Dattolo E, Ruocco M, Brunet C, Lorenti M and others (2014) Response of the seagrass *Posidonia oceanica* to different light environments: insights from a combined molecular and photo-physiological study. Mar Environ Res 101: 225–236

Demmig-Adams B, Adams WW III (1992) Photoprotection and other responses of plants to high light stress. Annu Rev Plant Physiol Plant Mol Biol 43:599–626

Demmig-Adams B, Adams WW III (1996) The role of xanthophyll cycle carotenoids in the protection of photosynthesis. Trends Plant Sci 1:21–26

Doney SC, Fabry VJ, Feely RA, Kleypas JA (2009) Ocean acidification: the other CO_2 problem. Annu Rev Mar Sci 1:169–192

Duarte CM (1991) Seagrass depth limits. Aquat Bot 40: 363–377

Duarte CM, Hendriks IE, Moore TS, Olsen YS and others (2013) Is ocean acidification an open-ocean syndrome? Understanding anthropogenic impacts on seawater pH. Estuaries Coasts 36:221–236

Eberhard S, Finazzi G, Wollman FA (2008) The dynamics of photosynthesis. Annu Rev Genet 42:463–515

Enríquez S, Duarte CM, Sand-Jensen K (1995) Patterns in the photosynthetic metabolism of Mediterranean macrophytes. Mar Ecol Prog Ser 119:243–252

Gattuso JP, Kirkwood W, Barry JP, Cox E and others (2014) Free-ocean CO_2 enrichment (FOCE) systems: present status and future developments. Biogeosciences 11: 4057–4075

Gieskes JM, Rogers WC (1973) Alkalinity determination in interstitial waters of marine sediments. J Sediment Res 43:272–277

Hanke GT, Holtgrefe S, König N, Strodtkötter I, Voss I, Scheibe R (2009) Use of transgenic plants to uncover strategies for maintenance of redox homeostasis during photosynthesis. Adv Bot Res 52:207–251

Hubbart S, Bird S, Lake JA, Murchie EH (2013) Does growth under elevated CO_2 moderate photoacclimation in rice? Physiol Plant 148:297–306

Hüner NPA, Bode R, Dahal K, Hollis L, Rosso D, Krol M, Ivanov AG (2012) Chloroplast redox imbalance governs phenotypic plasticity: the 'grand design of photosynthesis' revisited. Front Plant Sci 3:255

Jeffrey SW, Humphrey GF (1975) New spectrophotometric equations for determining chlorophylls *a*, *b*, c_1 and c_2 in higher plants, algae, and natural phytoplankton. Biochem Physiol Pflanz 167:191–194

Jones R, Ougham H, Thomas H, Waaland S (2012) The molecular life of plants. Wiley-Blackwell, Chichester

Kirk JTO (1994) Light and photosynthesis in aquatic ecosystems, Cambridge University Press, Cambridge

Koch EW, Barbier EB, Silliman BR, Reed DJ and others (2009) Non-linearity in ecosystem services: temporal and spatial variability in coastal protection. Front Ecol Environ 7:29–37

Lee KS, Park SR, Kim YK (2007) Effects of irradiance, temperature, and nutrients on growth dynamics of seagrasses: a review. J Exp Mar Biol Ecol 350:144–175

Li Y, Zhang Y, Zhang X, Korpelainen H, Berninger F, Li C (2013) Effects of elevated CO_2 and temperature on photosynthesis and leaf traits of an understory dwarf bamboo in subalpine forest zone, China. Physiol Plant 148:261–272

Lichtenthaler HK, Wellburn AR (1983) Determinations of total carotenoids and chlorophylls *a* and *b* of leaf extracts in different solvents. Biochem Soc Trans 11:591–592

Longstaff BJ, Dennison WC (1999) Seagrass survival during pulsed turbidity events: the effects of light deprivation on the seagrasses *Halodule pinifolia* and *Halophila ovalis*. Aquat Bot 65:105–121

McPherson ML, Zimmerman RC, Hill VJ (2015) Predicting carbon isotope discrimination in eelgrass (*Zostera marina* L.) from the environmental parameters — light, flow, and [DIC]. Limnol Oceanogr 60:1875–1889

Moore KA, Jarvis JC (2008) Environmental factors affecting recent summertime eelgrass diebacks in the lower Chesapeake Bay: implications for long-term persistence. J Coast Res (Spec Issue) 55:135–147

Moore KA, Shields EC, Parrish DB, Orth RJ (2012) Eelgrass survival in two contrasting systems: role of turbidity and summer water temperatures. Mar Ecol Prog Ser 448: 247–258

Niyogi KK (2000) Safety valves for photosynthesis. Curr Opin Plant Biol 3:455–460

Orth RJ, Carruthers TJB, Dennison WC, Duarte CM and others (2006a) A global crisis for seagrass ecosystems. Bioscience 56:987–996

Orth RJ, Luckenbach ML, Marion SR, Moore KA, Wilcox DJ (2006b) Seagrass recovery in the Delmarva Coastal Bays, USA. Aquat Bot 84:26–36

Ow YX, Uthicke S, Collier CJ (2016) Light levels affect carbon utilisation in tropical seagrass under ocean acidification. PLOS ONE 11:e0150352

Palacios SL, Zimmerman RC (2007) Response of eelgrass *Zostera marina* to CO_2 enrichment: possible impacts of climate change and potential for remediation of coastal habitats. Mar Ecol Prog Ser 344:1–13

Pfannschmidt T (2003) Chloroplast redox signals: how photosynthesis controls its own genes. Trends Plant Sci 8:33–41

Pfannschmidt T, Yang C (2012) The hidden function of photosynthesis: a sensing system for environmental conditions that regulates plant acclimation responses. Protoplasma 249:125–136

Pfannschmidt T, Bräutigam K, Wagner R, Dietzel L, Schröter Y, Steiner S, Nykytenko A (2009) Potential regulation of gene expression in photosynthetic cells by redox and energy state: approaches towards better understanding. Ann Bot 103:599–607

Ralph PJ, Polk SM, Moore KA, Orth RJ, Smith WO (2002) Operation of the xanthophyll cycle in the seagrass *Zostera marina* in response to variable irradiance. J Exp Mar Biol Ecol 271:189–207

Repolho T, Duarte B, Dionísio G, Paula JR and others (2017) Seagrass ecophysiological performance under ocean warming and acidification. Sci Rep 7:41443

Ruesink JL, Yang S, Trimble AC (2015) Variability in carbon availability and eelgrass (*Zostera marina*) biometrics along an estuarine gradient in Willapa Bay, WA, USA. Estuaries Coasts 38:1908–1917

Schneider G, Horta PA, Calderon EN, Castro C and others (2018) Structural and physiological responses of *Halodule wrightii* to ocean acidification. Protoplasma 255:629–641

Schubert N, Freitas C, Silva A, Costa MM and others (2018) Photoacclimation strategies in northeastern Atlantic seagrasses: integrating responses across plant organizational levels. Sci Rep 8:14825

Sisson GM, Shen J, Reay WG, Miles EJ, Kuo AYs, Wang HV (2010) The development of a management tool to assess bacterial impacts in Rudee Inlet, Virginia Beach. Virginia Institute of Marine Science, Dept. of Physical Sciences, Gloucester Point, VA

Smith RD, Pregnall AM, Alberte RS (1988) Effects of anaerobiosis on root metabolism of *Zostera marina* (eelgrass): implications for survival in reducing sediments. Mar Biol 98:131–141

Stark JS, Peltzer ET, Kline DI, Queirós AM and others (2019) Free Ocean CO_2 Enrichment (FOCE) experiments: scientific and technical recommendations for future *in situ* ocean acidification projects. Prog Oceanogr 172:89–107

van Heuven S, Pierrot D, Rae JWB, Lewis E, Wallace DWR (2011) MATLAB Program developed for CO_2 system calculations. Carbon Dioxide Information Analysis Center, Oak Ridge National Laboratory, Oak Ridge, TN

Vogelman TC, Nishio JN, Smith WK (1996) Leaves and light capture: light propagation and gradients of carbon fixation within leaves. Trends Plant Sci 1:65–70

Waldbusser GG, Salisbury JE (2014) Ocean acidification in the coastal zone from an organism's perspective: multiple system parameters, frequency domains, and habitats. Annu Rev Mar Sci 6:221–247

Walters RG (2005) Towards an understanding of photosynthetic acclimation. J Exp Bot 56:435–447

Yin ZH, Johnson GN (2000) Photosynthetic acclimation of higher plants to growth in fluctuating light environments. Photosynth Res 63:97–107

Zimmerman RC (2003) A biooptical model of irradiance distribution and photosynthesis in seagrass canopies. Limnol Oceanogr 48:568–585

Zimmerman RC (2006) Light and photosynthesis in seagrass meadows. In: Larkum AWD, Orth RJ, Duarte CM (eds) Seagrasses: biology, ecology and conservation. Springer Netherlands, Dordrecht, p 303–321

Zimmerman RC (2021) Scaling up: predicting the impacts of climate change on seagrass ecosystems. Estuaries Coasts 44:558–576

Zimmerman RC, Smith RD, Alberte RS (1987) Is growth of eelgrass nitrogen limited? A numerical simulation of the effects of light and nitrogen on the growth dynamics of *Zostera marina.* Mar Ecol Prog Ser 41:167–176

Zimmerman RC, Smith RD, Alberte RS (1989) Thermal acclimation and whole-plant carbon balance in *Zostera marina* L. (eelgrass). J Exp Mar Biol Ecol 130:93–109

Zimmerman RC, Kohrs DG, Steller DL, Alberte RS (1997) Impacts of CO_2 enrichment on productivity and light requirements of eelgrass. Plant Physiol 115:599–607

Zimmerman RC, Hill VJ, Gallegos CL (2015) Predicting effects of ocean warming, acidification, and water quality on Chesapeake region eelgrass. Limnol Oceanogr 60: 1781–1804

Zimmerman RC, Hill VJ, Jinuntuya M, Celebi B and others (2017) Experimental impacts of climate warming and ocean carbonation on eelgrass *Zostera marina.* Mar Ecol Prog Ser 566:1–15

Editorial responsibility: Emily Carrington, Friday Harbor, Washington, USA
Reviewed by: 3 anonymous referees

Submitted: November 20, 2020
Accepted: June 1, 2021
Proofs received from author(s): August 2, 2021